ELSEVIER

Coordination Chemistry Reviews
177 (1998) 3–35

COORDINATION CHEMISTRY REVIEWS

Organometallic complexes as luminescence probes in monitoring thermal and photochemical polymerizations

Alistair J. Lees *

Department of Chemistry, State University of New York at Binghamton, Binghamton, NY 13902-6016, USA

Received 29 May 1997; accepted 11 August 1997

Contents

Abstract

This review describes recent developments where several organometallic complexes have been employed as luminescence probes to monitor industrially important thermal and photochemical polymerization reactions. Both epoxy resin and acrylate thin-film materials are discussed. Attention is focused on polymer systems incorporating the metal complexes, $W(CO)_4L$ and *fac*-$XRe(CO)_3L$ (X = Cl, Br or I, and L is an α,α'-diimine ligand such as 2,2′-bipyridine or 1,10-phenanthroline, and related derivatives) which are shown to offer

* Tel.: + 1 607 7772362; fax: + 1 607 7774478; e-mail: alees@bingvmb.cc.binghamton.edu

PII S0010-8545(98)00099-X

considerable promise as spectroscopic probes. A key feature of these organometallic systems is that they are emissive from low-lying metal-to-ligand charge transfer (MLCT) excited states and that these energy levels are sensitive to environmental rigidity. The luminescence properties of these complexes in both solution and polymeric media are examined in detail and the photophysical parameters of the MLCT excited states are correlated with spectroscopic and rheological measurements acquired during the curing process of the polymer.

Keywords: Charge transfer; Curing; Electronic spectroscopy; Electronically excited states; Emission; Luminescence; Photophysical processes; Photopolymers; Polymerization; Polymers; Thermosetting polymers; Thin films; Transition metal organometallic compounds

1. Introduction

Environmental effects on electronic absorption spectra and luminescence properties of transition metal organometallic complexes are often substantial [1,2] and their solvatochromic characteristics have been studied in detail for a number of systems [3–20]. However, one of the most intriguing environmental features is the manner in which the emission bands of some of these complexes exhibit a distinct blue shift when the solution medium becomes rigid. This effect has been termed 'luminescence rigidochromism' [21,22] and has been observed for several metal carbonyl derivatives containing lowest energy metal-to-ligand charge transfer (MLCT) transitions. Usually, this phenomenon is seen when fluid solutions of these complexes are frozen to form rigid glasses [2,21–27]. Recently, the photophysical characteristics of several complexes exhibiting luminescence ridigochromism have been reviewed [28].

Over the past few years an interesting aspect of the luminescence rigidochromic effect has emerged, namely the use of emitting organometallic complexes as spectroscopic probes in monitoring the curing processes of both thermosetting and photosensitive polymers. During many polymerizations the solution environment obviously becomes very viscous and eventually quite rigid, and it is clear that a number of organometallic systems lend themselves as luminescence probes of these reactions. Indeed, as organometallic complexes are soluble in many different types of monomer/polymer solutions, their capability as spectroscopic probes could have widespread applications.

This review illustrates recent developments where luminescent organometallic complexes have been employed to monitor a variety of industrially important polymerizations. We primarily focus upon two metal carbonyl systems which emit from MLCT excited states and have demonstrated the most promise, to date, as spectroscopic probes; these are $W(CO)_4L$ and *fac*-$XRe(CO)_3L$, where L is an α,α'-diimine ligand such as 2,2′-bipyridine or 1,10-phenanthroline (and related derivatives) and X = Cl, Br or I. The spectroscopic features of these organometallic probe complexes (shown below) will be discussed in detail and compared to other

types of luminescence probes in polymers. Both thermosetting and photochemical polymerization reactions are reviewed.

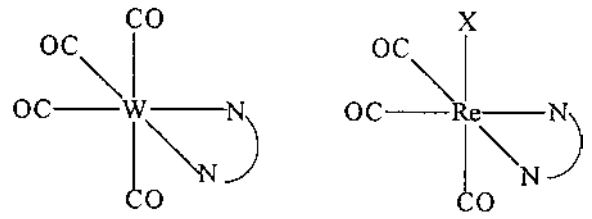

N N = 2,2′-bipyridine (bpy)
1-10-phenanthroline (phen)
(or derivatives)

X = Cl, Br or I

2. Electronic and photophysical properties

2.1. $W(CO)_4L$ complexes

The electronic characteristics of the $M(CO)_4(\alpha,\alpha'$-diimine) (M = Cr, Mo or W) system have been studied in considerable detail [12,23,24,29–32]. Fig. 1 illustrates electronic absorption spectra obtained from $W(CO)_4$(4-Me-phen) (4-Me-phen = 4-methyl-1,10-phenanthroline) in deoxygenated benzene at 293 K and in glassy EPA (ether/isopentane/ethanol, 5:5:2 by volume) solution at 80 K; these spectra are representative of the $M(CO)_4(\alpha,\alpha'$-diimine) series in both fluid and glass environments. At room temperature the spectrum of $W(CO)_4$(4-Me-phen) is dominated by an intense MLCT absorption band that is centered at 500 nm ($\varepsilon_{max} = 9250\ M^{-1}\ cm^{-1}$), whereas weaker ligand field (LF) transitions are also observable at 391 nm (sh) and 340 nm ($\varepsilon_{max} = 3550\ M^{-1}\ cm^{-1}$) [23]. The lowest energy MLCT absorption features of $W(CO)_4$(4-Me-phen) and those of a number of closely related derivatives are recognized to be especially solvent dependent [12,16]. Also noticeable is that upon cooling the solution to low temperature and forming a frozen glass the MLCT band envelope substantially blue shifts, undergoes band sharpening and reveals a structure depicting two MLCT features (see Fig. 1).

A detailed series of resonance Raman (RR) and magnetic circular dichroism (MCD) measurements has been carried out on the $M(CO)_4(\alpha,\alpha'$-diimine) system and these indicate that the lowest energy absorption actually comprises three MLCT transitions. The most intense one has been established as a z-polarized $(d_{yz})b_2 \rightarrow b_2$ (π^*) transition that is directed along the dipole vector of the complex [30,32]. Additionally, the solvatochromism exhibited by these complexes has been

associated with the $b_2 \rightarrow b_2^*$ transition and, specifically, with the extent of mixing that exists between the metal d_{yz} and ligand π^* orbitals. For $W(CO)_4$(4-Me-phen), the degree of mixing between these metal and ligand orbitals is fairly small and the complex is extremely sensitive to variations in solvent [12,16,23,24,29,32]. In contrast to the bpy and phen derivatives, though, the amount of mixing of the corresponding orbitals in other α,α'-diimine species such as $W(CO)_4$(R-dab) and $W(CO)_4$(R-pyca) (R-dab = 1,4-diaza-1,3-butadiene and R-pyca = pyridine-2-carbaldehyde imine) is considerably lower and the solvent dependence is also much smaller.

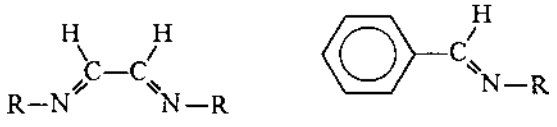

R-dab R-pyca

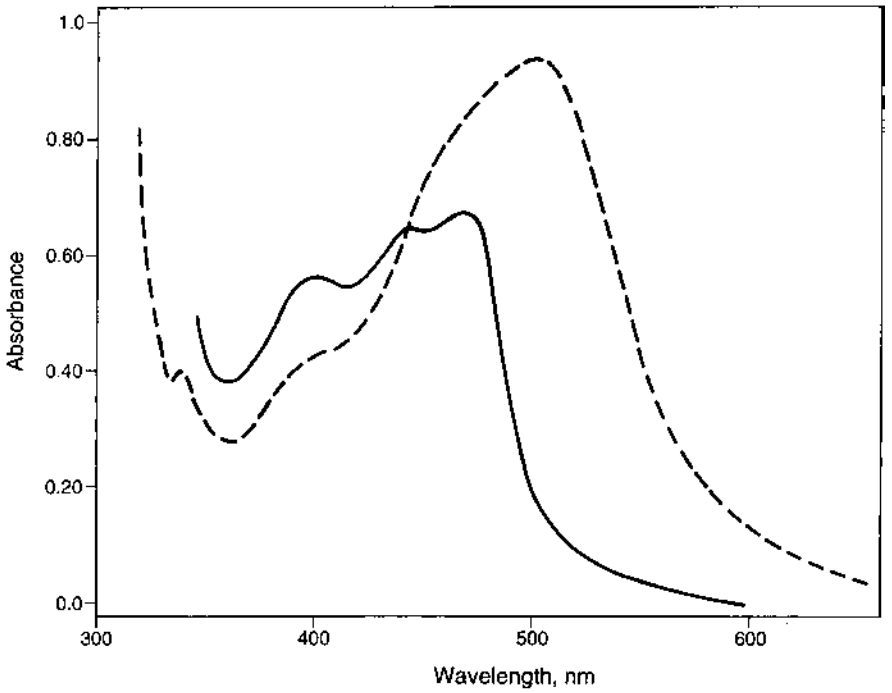

Fig. 1. Electronic absorption spectra of $W(CO)_4$(4-Me-phen) in (– – –) deoxygenated benzene at 293 K and (——) an EPA glass at 80 K. (Adapted, with permission, from Refs. [23,24].)

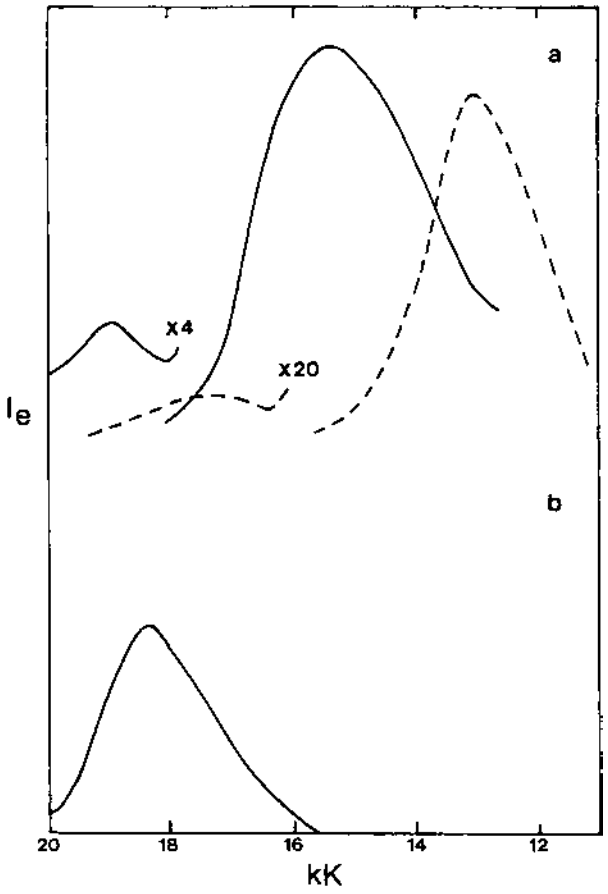

Fig. 2. Emission spectra of (a) $W(CO)_4$(4-Me-phen) and (b) $W(CO)_4$(en) in (– – –) deoxyygenated benzene at 293 K and (——) EPA glasses at 80 K. Excitation wavelength is 400 nm. The spectrum at 293 K is uncorrected whereas the spectra at 80 K are fully corrected for wavelength variations in detector response (the emission intensity at low temperature is approximately 100 times more intense than that at room temperature). No luminescence was observed from $W(CO)_4$(en) at room temperature. (Reprinted, with permission, from Ref. [24].)

The RR excitation profiles of $M(CO)_4$(α,α'-diimine) have identified additional y-polarized $(d_{x^2-z^2})a_1 \rightarrow b_2(\pi*)$ and x-polarized $(d_{xy})a_2 \rightarrow b_2$ (π^*) MLCT transitions in the band envelope, although the latter component is relatively weak for a substituted phen derivative [32]. Therefore, the absorption features observed on forming the frozen glassy solution of $W(CO)_4$(4-Me-phen) at 80 K (see Fig. 1) are entirely in accordance with these assignments. The most intense MLCT components at low temperature, appearing at 444 and 468 nm, are associated with the $a_1 \rightarrow b_2^*$ and $b_2 \rightarrow b_2^*$ transitions, respectively.

Emission spectra observed from the $M(CO)_4$(α,α'-diimine) system reveal several important photophysical aspects. Data recorded from $W(CO)_4$(4-Me-phen) are

typical of the bpy and phen series; Fig. 2 illustrates spectra obtained from the complex in deoxygenated benzene at 293 K and an EPA glass at 80 K [24]. Dual ^{3}MLCT emission bands, representing a weak higher energy feature and a more intense lower energy band, are observable at either temperature. The intensity ratio of these bands remains virtually unchanged when an EPA solution is cooled from 293 to 150 K, but once the solution passes through the glass transition temperature (120–140 K) and reaches 80 K the overall emission intensity increases ca. 100-fold, the lower band becomes even more dominant and both bands undergo a discernible blue shift. The latter phenomenon, known as luminescence rigidochromism [21,22], is particularly significant for the lower energy band. Emission has also been detected from $W(CO)_4$(en) (en = ethylenediamine) at 80 K and illustrates the close position of the ^{3}LF excited state; this emission spectrum is included in Fig. 2 for comparison purposes. A summary of the luminescence maxima observed for a range of $M(CO)_4(\alpha,\alpha'$-diimine) complexes is shown in Table 1.

The dual luminescence spectra exhibited by $M(CO)_4(\alpha,\alpha'$-diimine) in room temperature solution are unusual and have been studied as a function of excitation wavelength [24]. As shorter exciting wavelengths are used, the higher energy emission band is seen to increase substantially in intensity (see Fig. 3). From detailed studies of the emission and excitation data it has been concluded that the ^{3}MLCT emitting levels are in thermal equilibrium with each other in fluid solution. Upon forming the frozen glass, however, the thermal equilibration is lost and the ^{3}MLCT states emit independently. The ^{3}LF emission is also present at 80 K and is likely the reason for the reduced rigidochromic shift displayed by the higher energy band.

A comparison of the luminescence properties of $W(CO)_4$(4-Me-phen) with those of other $M(CO)_4(\alpha,\alpha'$-diimine) complexes illustrates further aspects of the photophysical deactivation mechanism [32]. Emission spectra have been recorded from $W(CO)_4$L (L = 4,7-Ph_2-phen, *i*-Pr-pyca and *i*-Pr-dab) in benzene at 293 K and 2-Me-THF (2-methyl-tetrahydrofuran) at 80 K; these results are depicted in Fig. 4.

Table 1
Emission maxima of $M(CO)_4(\alpha,\alpha'$-diimine) complexes in various solutions[a]

Complex	λ_{em} (nm)		
	Benzene, 293 K	EPA, 293 K	EPA, 80 K
$Mo(CO)_4$(4-Me-phen)	546, 752	553, 765	533, 647
$Mo(CO)_4$(5-Me-phen)	568, 764	572, 772	530, 658
$Mo(CO)_4$(4,7-Ph_2-phen)	582, 770	585, 785	545 (sh), 660
$Mo(CO)_4$(en)	[b]	[b]	[b]
$W(CO)_4$(4-Me-phen)	585, 782	584, >780	527, 677
$W(CO)_4$(4,7-Ph_2-phen)	595, 780	595, >800	550 (sh), 675
$W(CO)_4$(en)	[b]	[b]	542

[a] Data taken from Ref. [24]. Excitation wavelength is 400 nm, and the spectra are fully corrected for wavelength variations in detector response; sh = shoulder.
[b] No emission observed.

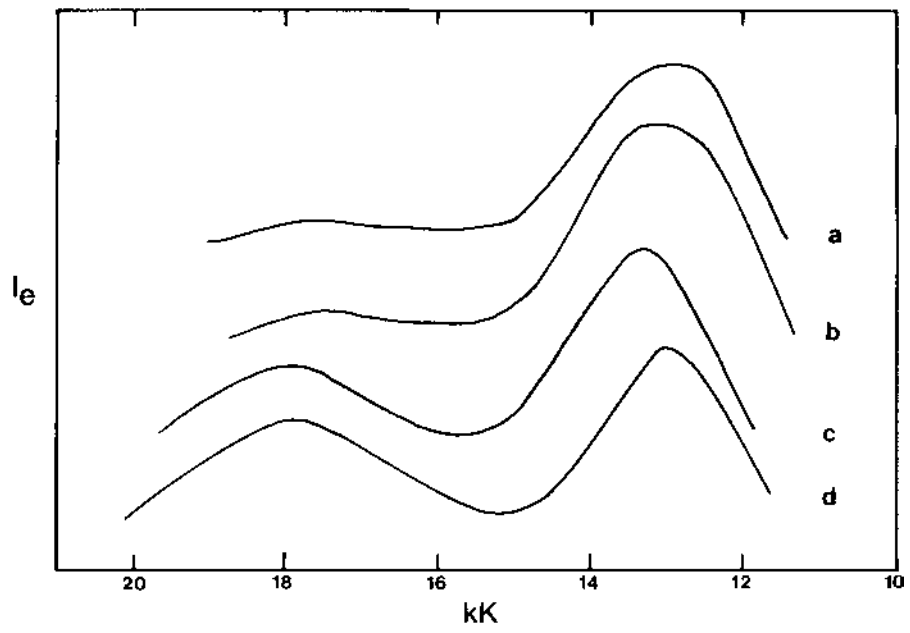

Fig. 3. Emission spectra of $W(CO)_4$(4-Me-phen) in deoxygenated benzene at 293 K. Excitation wavelengths are: (a) 475, (b) 450, (c) 400 and (d) 350 nm. The spectra are uncorrected for detector response; the lowest energy band is slightly blue shifted on 400 nm excitation due to interference from solvent scatter. (Reprinted, with permission, from Ref. [24].)

The $W(CO)_4$(4,7-Ph_2-phen) complex exhibits emission features similar to the $W(CO)_4$(4-Me-phen) derivative. The room temperature spectra of the corresponding *i*-Pr-pyca and *i*-Pr-dab complexes, however, were determined to be dependent on the excitation wavelength, revealing the presence of two emitting levels in these apparently single emission bands. On lowering the temperature to 80 K, though, the luminescence spectrum of $W(CO)_4$(*i*-Pr-dab) exhibits only a low energy feature, resembling that in the bpy and phen complexes. In contrast, the luminescence spectrum of $W(CO)_4$(*i*-Pr-dab) undergoes hardly any change upon cooling to 80 K.

Clearly, the emission spectra are also greatly influenced by the MLCT character of the *z*-polarized ($b_2 \rightarrow b_2^*$) transition. The mixing of the metal d_{yz} and ligand π^* orbitals is much larger in the dab complexes than in the bpy or phen derivatives, but the mixing in the pyca complexes lies somewhat in between [32,33]. RR excitation profiles have indicated that MLCT $b_2 \rightarrow b_2^*$ excitation mainly affects the metal skeletal vibrations of the R-dab complexes, whereas it is the internal vibrations of the α,α'-diimine ligands which are mostly affected in the bpy and phen derivatives. Consequently, it is concluded that the R-dab complexes undergo efficient nonradiative decay (and an absence of the lowest energy band) as these metal–ligand skeletal modes most strongly influence the electronic integral and, thus, the matrix element connecting the ground and excited states [34].

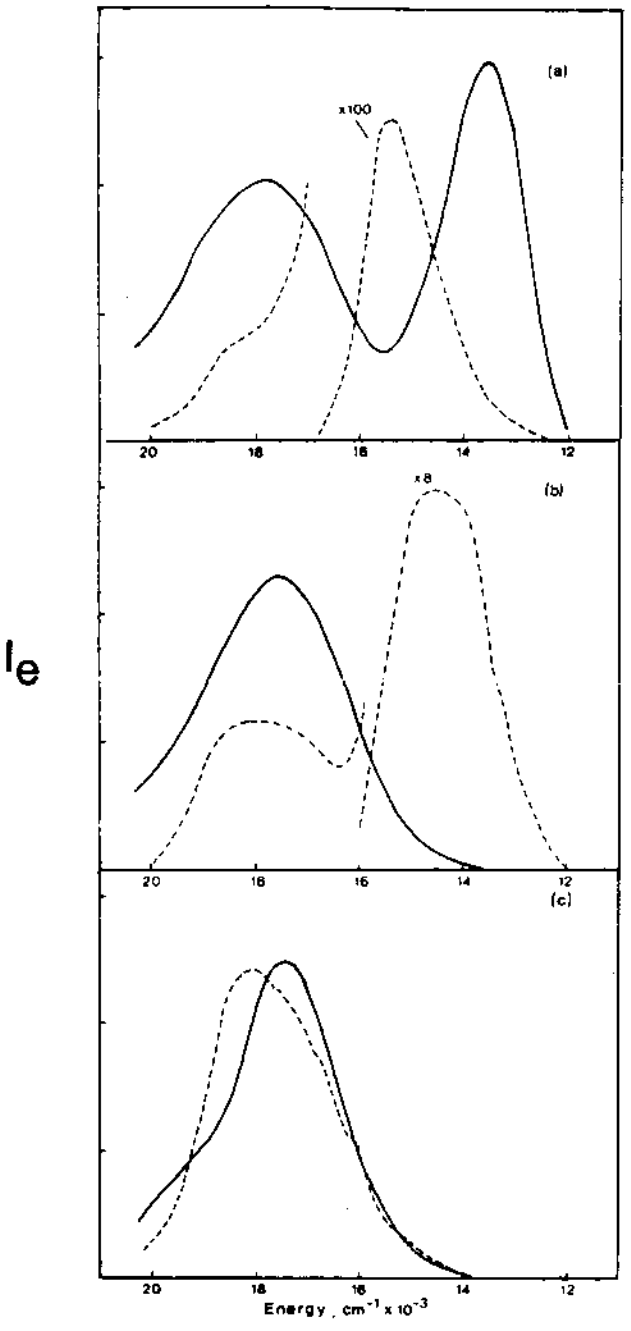

Fig. 4. Emission spectra of (a) $W(CO)_4$(4,7-Ph_2-phen), (b) $W(CO)_4$(i-Pr-pyca), and (c) $W(CO)_4$(i-Pr-dab) in (——) benzene at 293 K and (– – –) a 2-Me-THF glass at 80 K. Excitation wavelength is 488 nm. (Reprinted, with permission, from Ref. [32].)

RR excitation profiles of the $W(CO)_4$(*i*-Pr-pyca) complexes reveal that the $b_2 \rightarrow b_2^*$ transition has intermediate MLCT character and indeed these molecules behave photophysically like the R-dab derivatives in room temperature solution. In a rigid environment at low temperature, however, the nonradiative deactivation processes are reduced and the emission spectra are similar to the bpy and phen complexes [32]. Solvent dependence studies of the excitation spectra have further confirmed the highly solvatochromic nature of the *z*-polarized $b_2 \rightarrow b_2^*$ transition in the lowest energy ^{3}MLCT emission feature of the $M(CO)_4(\alpha,\alpha'$-diimine) system.

2.2. *fac*-$XRe(CO)_3L$ complexes

The electronic and photophysical properties of the *fac*-$XRe(CO)_3L$ system have been extensively investigated following the discovery that their lowest energy excited states exhibit readily detectable luminescence in the visible region in several environments, including room temperature solution. Indeed, the first observation of luminescence rigidochromism was reported for a series of *fac*-$ClRe(CO)_3L$ (L = bpy, phen, 5-Me-phen, 4,7-Ph_2-phen, 5-Cl-phen, 5-Br-phen, 5-NO_2-phen, phen-5,6-dione and biquin) derivatives [21]. The ligands here each possess an empty low-lying π^*-acceptor orbital and the complexes themselves exhibit intense MLCT absorption bands. The emission from these complexes has, therefore, been associated with these lowest energy MLCT excited states.

Representative electronic absorption and emission spectra are shown in Fig. 5 for *fac*-$ClRe(CO)_3$(phen) in EPA at 298 and 77 K [21]. It is noticeable that the MLCT

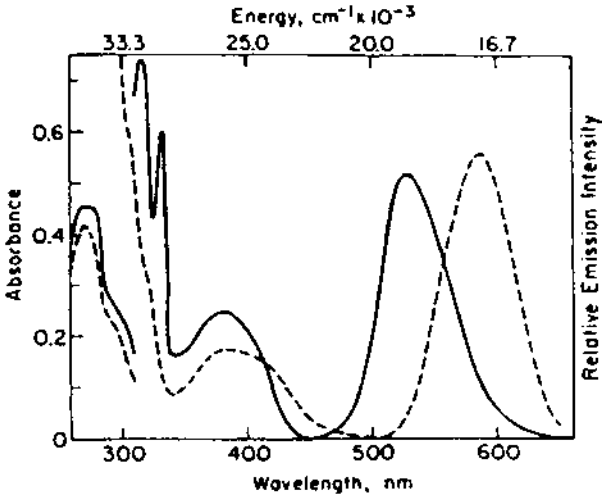

Fig. 5. Electronic absorption (left) and emission (right) spectra of *fac*-$ClRe(CO)_3$(phen) in EPA at (– – –) 298 K and (——) 77 K. Room temperature absorption maxima are 26100 cm^{-1} ($\varepsilon = 4000$ M^{-1} cm^{-1}) and 37030 cm^{-1} ($\varepsilon = 30600$ M^{-1} cm^{-1}); the low temperature spectrum is not corrected for solvent contraction. Emission spectra at 298 and 77 K were not recorded at the same sensitivity. (Reprinted, with permission, from Ref. [21].)

Table 2
Emission properties of *fac*-$ClRe(CO)_3L$ complexes[a]

L	Emission max (10^{-3} cm^{-1})		τ_e (μs)		$\phi_e(\pm 15\%)$[c]	ϕ_e ($\pm 15\%$)
	298 K	77 K	298 K	77 K	298 K	77 K
phen	17.33	18.94	0.3	9.6	0.036	0.33
bpy		18.87	0.6	3.8		
5-Me-phen	17.01	18.83	<0.65	5.0	0.030	0.30
4,7-Ph_2-phen	17.24	18.18	0.4	11.25		
5-Cl-phen	17.12	18.69	<0.65	6.25		
5-Br-phen	17.12	18.69	<0.65	7.6	0.020	0.20
5-NO_2-phen	[b]	18.28		11.8		0.033
phen-5,6-dione	[b]	18.45		2.5		
biquin[c]	[b]	14.58				

[a] Data taken from Ref. [21]. Measurements in EPA at 77 K or in CH_2Cl_2 at 298 K.
[b] Luminescence was not detectable from these complexes in solution at 298 K.
[c] Quantum yields determined in benzene at 298 K.

emission band is moved substantially to higher energy upon forming the rigid glass, whereas the MLCT absorption band is shifted considerably less. The emission characteristics for the above series of *fac*-$ClRe(CO)_3L$ complexes are summarized in Table 2 [21]. Both emission quantum yields (ϕ_e) and lifetimes (τ_e) are increased significantly when the solution is cooled to 77 K and forms a frozen glass, implying that the radiative decay pathways are favored in the rigid environment. For each of the complexes giving rise to luminescence in fluid solution there is a distinct blue shift in the emission maximum (on the order of 940–1820 cm^{-1}) when the glassy matrix is formed.

The nature of the MLCT excited state in the *fac*-$XRe(CO)_3L$ system has been further explored using a variety of spectroscopic techniques. Time-resolved resonance Raman measurements of *fac*-$XRe(CO)_3$(bpy) (X = Cl or Br) have provided strong evidence for the $Re \rightarrow \pi^*$(bpy) assignment of the lowest energy excited state [35]. Intense excited state Raman lines have been observed that are associated with the radical anion of bpy, and the amount of charge transferred from Re to bpy in the lowest energy excited state has been calculated to be 0.84 [36]. Fast time-resolved infrared spectroscopy has been used to probe the vibrational spectrum of the excited states of *fac*-$ClRe(CO)_3$(bpy) and the closely related *fac*-$XRe(CO)_3$(4,4′-bpy)$_2$ (X = Cl or Br) complexes. These spectra each reveal a shift in the carbonyl stretching bands to higher frequency relative to the ground state which is concordant with electron transfer to the bipyridyl ligands and oxidation of the metal center [37–40].

There is also evidence that the MLCT emitting levels in metal carbonyl complexes such as *fac*-$XRe(CO)_3L$ are mainly of triplet character [1,2], although it is recognized that the heavy metal in these complexes precludes a pure multiplicity designation [41]. For example, in *fac*-$ClRe(CO)_3$(phen) the emission is quenched by

the triplet levels of anthracene [42] and *trans*-stilbene [43]; these energy transfers take place via collisional processes [21]. In the case of stilbene, a *trans*→*cis* isomerization occurs too, further illustrating that it is the triplet excited state of *trans*-stilbene which is implicated in the quenching mechanism [44]. Additionally, the observed *trans*→*cis* isomerization yields for the stilbene are equivalent to those obtained for the benzophenone sensitization of *trans*-stilbene [43], illustrating that the efficiency of intersystem crossing in these Re complexes is close to unity [21,45].

A comparison of the energy shifts observed in the absorption and emission bands (see Fig. 5 and Table 2) reveals that it is predominantly the ^{3}MLCT excited states which are subjected to the rigidochromism and the effect on the corresponding ^{1}MLCT levels is much smaller. Environmental influences on the MLCT absorption and emission bands are shown in Table 3 for several *fac*-ClRe(CO)$_3$L complexes [21]. It is clear that the luminescence rigidochromism is associated with the rigidity change in the medium rather than simply being a temperature effect. Each of the complexes exhibits a substantial blue shift in its emission band (of up to 1830 cm^{-1}) when the solution becomes rigid. Even at room temperature significant hypsochromic shifts occur when the rhenium system is incorporated in a rigid polyester resin.

Table 3
Environmental effects on MLCT absorption and emission maxima of *fac*-ClRe(CO)$_3$L complexes[a]

L	Environment	Absorption max (10^{-3} cm^{-1})	Emission max (10^{-3} cm^{-1}) [τ_e (μs)]
phen	CH_2Cl_2, 298 K	26.53	17.33 (0.3)
	Polyester resin, 298 K		18.52 (3.67)
	EPA, 77 K		18.94 (9.6)
5-Me-phen	Benzene, 298 K	25.65	17.00 ($\leqslant$0.65)
	CH_2Cl_2, 298 K	26.32	17.01
	CH_3OH, 298 K	27.05	17.00
	Pure solid, 298 K		18.42
	Polyester resin, 298 K		18.48 (3.5)
	EPA, 77 K		18.83 (5.0)
5-Br-phen	Benzene, 298 K	25.32	17.15 ($\leqslant$0.65)
	CH_2Cl_2, 298 K	25.84	17.12
	CH_3OH, 298 K	26.88	17.04
	Pure solid, 298 K		17.83
	Polyester resin, 298 K		18.32 (2.2)
	EPA, 77 K		18.69 (7.6)
5-Cl-phen	CH_2Cl_2, 298 K	25.91	17.12
	Pure solid, 298 K		17.99
	EPA, 77 K		18.69 (6.25)

[a] Data taken from Ref. [21].

3. Photosensitive polymers

UV-curable coatings are employed extensively in medicine and dentistry and in a variety of industries such as microelectronics, graphic arts and packaging. Acrylate-based thin films are used widely, for instance, as photoresist materials during the manufacture of computer boards [46–48]. In all of these applications, though, it is highly desirable to know details of the physical state throughout the polymer curing process.

Several fluorescence probe systems have been used to spectroscopically follow the curing kinetics of thermosetting materials [49–52], but for only a few cases have these been shown useful in monitoring photochemical polymerizations [53,54]. Usually, the absorption and emission bands of traditional fluorescence probe molecules significantly interfere with the spectral features of the photoinitiators. A number of experimental approaches have been taken to circumvent this particular problem. One involves the use of multiple fluorescence systems where the nonradiative relaxation rates are subject to the ability of the probe molecule to undergo rotation [55–60]. Another is to use fluorescence probes in which the formation of the polymeric network influences an energy transfer mechanism to a quencher molecule [61–63]. Additionally, the generation of excimers (typically pyrene or pyrene derivatives) during the polymerization is able to provide a shift in the position of the emission band and, hence, a spectroscopic probe of the process [64–70]. Lately, the application of fluorescence probes to monitor polymer formation has been reviewed [71].

3.1. Acrylate-based films

Luminescent organometallic complexes have also recently been demonstrated to be useful as spectroscopic probes in the cross-linking polymerization of photosensitive thin films. The $W(CO)_4(\alpha,\alpha'$-diimine) and *fac*-$XRe(CO)_3(\alpha,\alpha'$-diimine) systems both exhibit significant spectral changes during acrylate polymerizations. These metal complexes possess a number of physical and spectroscopic properties that lend themselves useful in this regard. Firstly, the complexes are soluble and thermally stable in nonpolar solutions containing the monomer. Secondly, the complexes exhibit low-lying MLCT absorption bands which facilitate excitation in the visible region that is significantly removed from the photoinitiator absorption. Thirdly, these MLCT absorption bands are intense which necessitates only a low concentration (typically $< 0.5\%$ by weight) of the probe molecule in the resin. Fourthly, the emission of the probe complex appears at very long wavelength and quite distinct from the spectral features of any of the monomer/polymer and photoinitiator components. Finally, the emission from the organometallic complex is sensitive to rigidity changes taking place during the polymerization.

Results obtained from the $W(CO)_4$(4-Me-phen) complex illustrate these key spectroscopic features [72]. Fig. 6 depicts electronic absorption spectra recorded from a 0.25 mm thickness film of a photosensitive acrylate system comprising a 1:1 (by weight) ratio of trimethylolpropane triacrylate (TMPTA) and medium weight

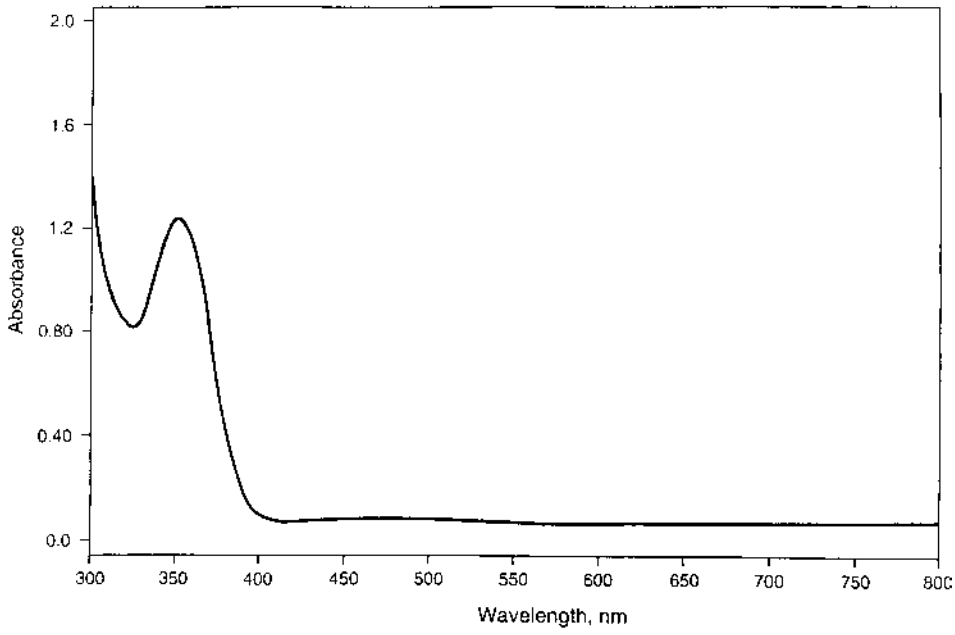

Fig. 6. Electronic absorption spectrum of a 1:1 (by weight) TMPTA/PMMA 0.25 mm thin film containing benzophenone photoinitiators and 0.3% (by weight) $W(CO)_4$(4-Me-phen) at 293 K. (Reprinted, with permission, from Ref. [72].)

poly(methyl methacrylate) (PMMA). To this thin film has been incorporated the photoinitiators benzophenone (4% by weight) and 4,4′-bis(dimethylamino)benzophenone (0.5% by weight) and the probe complex $W(CO)_4$(4-Me-phen) (0.3% by weight). The major absorption band from this acrylate film appearing at 353 nm is due to the added photoinitiators. The organometallic complex is present in such a low concentration that its normally intense MLCT absorption transitions are barely detectable ($A < 0.1$) in the visible region between 400 and 550 nm. Notably, on exposing the acrylate thin film to UV light this spectrum was found not to change, indicating that the metal complex does not photodecompose during the polymerization. Although $W(CO)_4$(4-Me-phen) exhibits photoreactive LF states in the UV region, these absorptions are weak and completely masked by the intense photoinitiator absorption bands.

Luminescence spectra recorded on 400 nm excitation from the same composition of TMPTA/PMMA thin film at 293 K are shown in Fig. 7. Before UV irradiation, the characteristic dual ^{3}MLCT emission features of $W(CO)_4$(4-Me-phen) are observable at 520 and 750nm, and the spectrum is similar to that determined in fluid solution (Figs. 2 and 3). After UV irradiation for 60 s, though, the two ^{3}MLCT emission bands become almost equivalent in intensity and their maxima have shifted to 525 and 715 nm, respectively. In the absence of added $W(CO)_4$(4-Me-phen) the unirradiated thin film gives rise to no detectable emission in the 450–800

nm region; however, following UV irradiation substantial scattered light is observed in the 420–620 nm region. Therefore, the gain in intensity of the short wavelength emission component is associated with both the ^{3}MLCT emission and an increase in scattered light from the polymer surface. In contrast, the long wavelength emission band is attributed solely to the ^{3}MLCT emission of the $W(CO)_4$(4-Me-phen) complex.

The changes in intensity of this long wavelength emission band of $W(CO)_4$(4-Me-phen) in the TMPTA/PMMA thin film have been monitored at several irradiation times (Fig. 8). Immediately upon excitation there is a steep increase in the emission intensity, followed by a more gradual change, finally reaching a plateau after ca. 60 s of UV irradiation. A similar dependence is observed in the decline of the infrared band at 808 cm^{-1}, corresponding to the CH_2 wagging mode of the acrylate monomer. Hence, the emission changes displayed by the metal complex are able to reflect the extent to which the acrylate monomer is consumed during the photopolymerization. Significantly, in the absence of added photoinitiator the emission intensity of the long wavelength ^{3}MLCT emission band remains constant, providing further evidence that the organometallic complex does not undergo degradation during the polymerization or itself act as a photoinitiator in these acrylate films.

The *fac*-$XRe(CO)_3(\alpha,\alpha'$-diimine) system has also been successfully employed as a spectroscopic probe of acrylate polymerization [73–75]. Fig. 9 illustrates emission

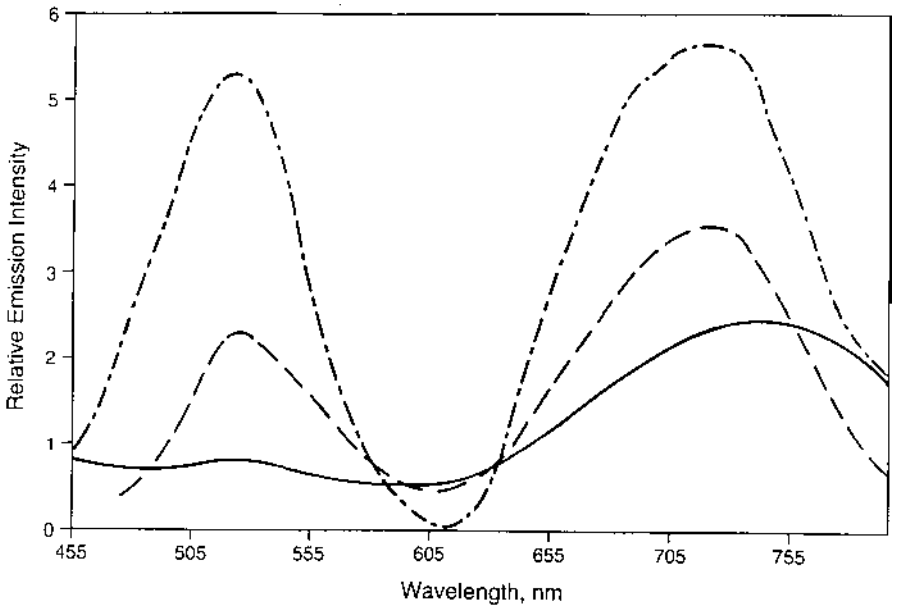

Fig. 7. Emission spectra of a 1:1 (by weight) TMPTA/PMMA 0.25 mm thin film containing benzophenone photoinitiators and 0.3% (by weight) $W(CO)_4$(4-Me-phen) following (——) 0 s, (– – –) 10 s, and (– - –) 60 s UV exposure at 293 K. Excitation wavelength is 400 nm in each case. (Reprinted, with permission, from Ref. [72].)

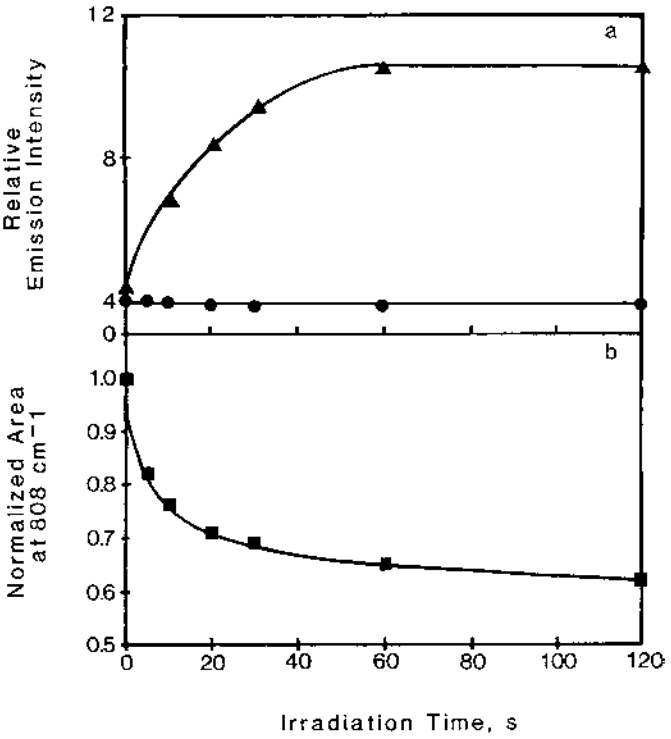

Fig. 8. (a) Plots of emission intensity at 715 nm of 0.3% (by weight) $W(CO)_4$(4-Me-phen) in a 1:1 (by weight) TMPTA/PMMA 0.25 mm thin film as a function of UV irradiation time (▲) with and (●) without the benzophenone photoinitiators. Excitation wavelength is 400 nm in each case. (b) Plot of the normalized area of acrylate monomer vibration at 808 cm^{-1} in a 1:1 (by weight) TMPTA/PMMA 0.25 mm thin film as a function of UV irradiation time. (Reprinted, with permission, from Ref. [72].)

spectra recorded from a 0.25 mm thickness film of 1:1 (by weight) TMPTA/PMMA with incorporation of photoinitiator 2,2-dimethoxy-2-phenylacetophenone (1% by weight) and probe complex *fac*-$ClRe(CO)_3$(4,7-Ph_2-phen) (0.01% by weight) [74]. Once again, the intensity of the ^{3}MLCT emission band increases substantially during the course of the acrylate cross-linking reaction. The emission band undergoes a distinct hypsochromic shift, moving from 576 nm (before irradiation) to 562 nm (after 120 s of irradiation). Additionally, the emission lifetime of the complex increases from 0.85 μs in the unirradiated film to 2.5 μs in the film that has been exposed to UV light for 120 s.

Radiative (k_r) and nonradiative (k_{nr}) relaxation rate constants can be derived by interrelating the experimental emission quantum yield (ϕ_e) and emission lifetime (τ_e) data, according to Eqs. (1) and (2). As indicated by the above emission results, both the emission intensity and lifetime values were observed to increase approximately by a factor of three on acrylate polymerization; thus, it can be deduced from Eq. (1) that there is actually little change in k_r during the cross-linking process.

Apparently, the higher emission intensity and lifetime values are predominantly due to a reduction in k_{nr}. This photophysical effect can be qualitatively related to changes in vibrational and rotational nonradiative relaxation pathways brought about by the increasing rigidity of the polymer environment and the corresponding lowering of the matrix free volume.

$$k_r = \phi_e/\tau_e \tag{1}$$

$$k_{nr} = (1/\tau_e) - k_r \tag{2}$$

Earlier work on paraffins, rhodamine dyes and 1,3-bis(*N*-carbazolyl)propane excimers has also established that there is a relationship between k_{nr} and polymer viscosity and free volume [76–78]. Furthermore, this dependence has been explored in the context of decreasing free volume during methyl methacrylate polymerization [79,80]. In general, these studies have illustrated that the nonradiative decay processes follow an exponential relationship with polymer free volume (v_f), in which k_{nr} reduces as free volume is decreased [see Eq. (3)]. Here, k°_{nr} is the intrinsic rate

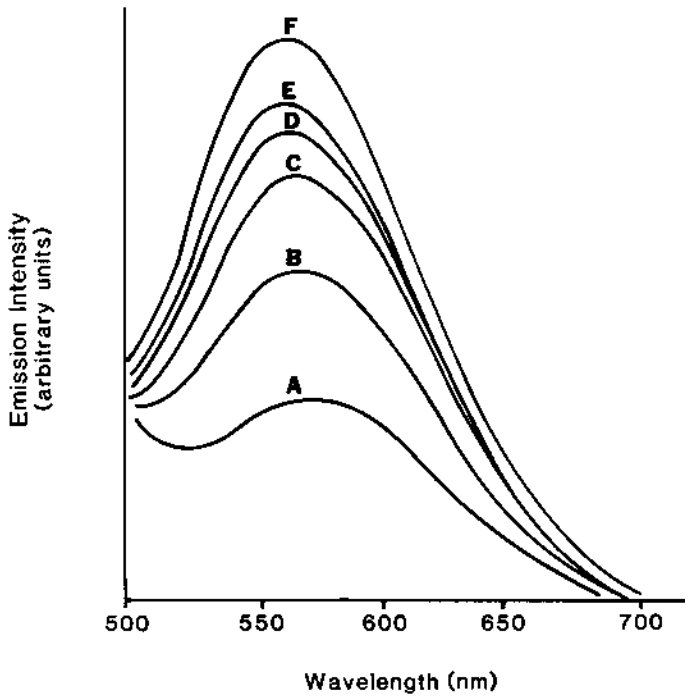

Fig. 9. Emission spectra at 293 K of a 1:1 (by weight) TMPTA/PMMA 0.25 mm thin film containing an acetophenone photoinitiator and 0.01% (by weight) *fac*-$ClRe(CO)_3(4,7\text{-}Ph_2\text{-phen})$ as a function of UV exposure time: (A) 0 s, (B) 5 s, (C) 10 s, (D) 20 s, (E) 30 s and (F) 60 s. The emission spectra are uncorrected for photomultiplier response; excitation wavelength is 420 nm in each case. (Reprinted, with permission, from Ref. [74].)

Table 4
Emission data of *fac*-ClRe(CO)$_3$(4,7-Ph$_2$-phen) in the photosensitive acrylate system as a function of resin composition[a]

PMMA:TMPTA ratio (wt.%)	λ_{em} (nm)		ΔE^{c}_{em} (cm^{-1})	I_f/I^{d}_o
	Uncured resin	Cured[b] resin		
30:70	583	561	672	6.9
40:60	580	561	584	4.6
50:50	576	562	432	2.5
60:40	567	562	160	2.1

[a] Data taken from Ref. [75]. Emission maxima are uncorrected for photomultiplier response; excitation wavelength is 420 nm.
[b] Following UV light exposure for 120 s.
[c] Energy difference of the MLCT band maxima in the uncured and cured materials.
[d] Ratio of the initial (I_o) and final (I_f) emission intensities recorded at the MLCT band maxima.

of molecular nonradiative relaxation, v_o is the van der Waals volume of the probe molecule, and b is a constant that is particular to the probe species.

$$k_{nr} = k^{\circ}_{nr} \exp(-v_o/bv_f) \quad (3)$$

Consequently, the experimentally observed changes in both emission intensity and lifetime for *fac*-ClRe(CO)$_3$(4,7-Ph$_2$-phen) in the TMPTA/PMMA thin film are entirely in accordance with this interpretation.

The determined hypsochromic shifts in the emission bands of both the W(CO)$_4$L and *fac*-XRe(CO)$_3$L systems in the acrylate polymerization are analogous to those exhibited in solution on forming a frozen glass (vide supra) and, hence, they appear to also be related to the luminescence rigidochromic effect. Various compositions of PMMA:TMPTA have been investigated with the *fac*-ClRe(CO)$_3$(4,7-Ph$_2$-phen) probe and these results are summarized in Table 4. The magnitudes of the rigidochromic shift (ΔE_{em}) and the intensity ratio (I_f/I_o) of the probe emission (where I_f is the intensity of the ^{3}MLCT emission band after 120 s of UV light excitation and I_o is the emission intensity prior to light exposure) are both reduced when the starting mixture has a higher PMMA content. These changes can be rationalized, however, if one recognizes that the viscosity of the initial resin is raised when the ratio of PMMA to TMPTA is increased, so the net viscosity change on curing the resin will be less.

3.2. Epoxy-based films

The *fac*-ClRe(CO)$_3$(4,7-Ph$_2$-phen) complex has been shown to be a useful spectroscopic probe in the curing of photosensitive epoxy-based materials [74]. Fig. 10

illustrates emission spectra obtained from a 0.05 mm thickness film of a mixed epoxy system of bisphenol A/novalac resin and diglycidyl ether of bisphenol A (DGEBA) containing cation-generating triarylsulfonium hexafluoroantimonate salts as photoinitiators and 0.005% (by weight) of the organometallic probe complex *fac*-$ClRe(CO)_3(4,7\text{-}Ph_2\text{-phen})$.

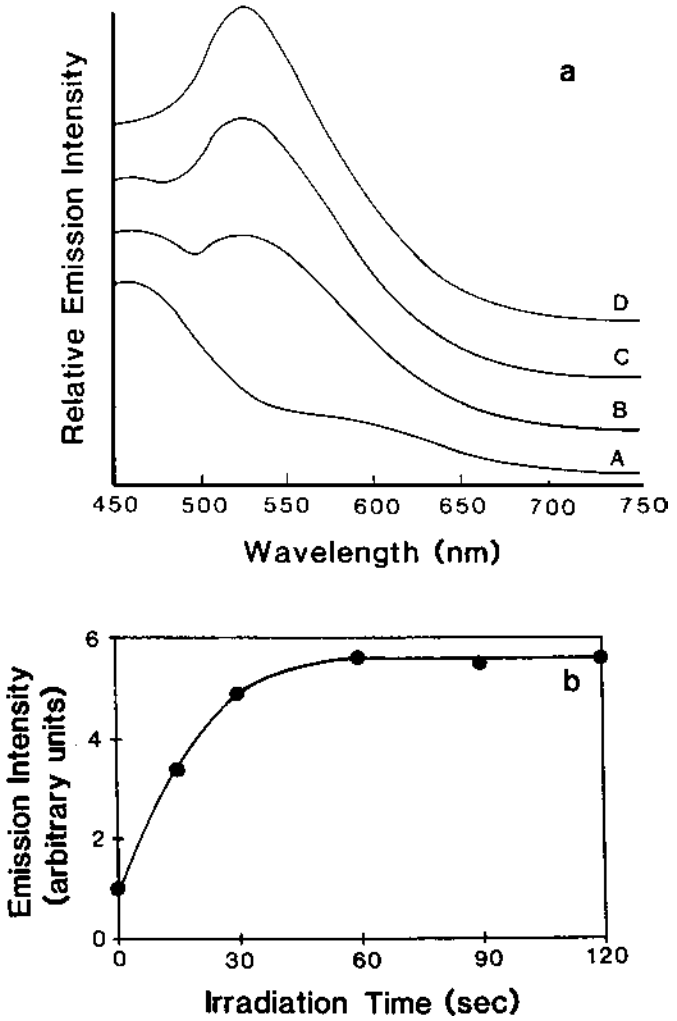

Fig. 10. (a) Emission spectra at 293 K of 0.005% (by weight) *fac*-$ClRe(CO)_3(4,7\text{-}Ph_2\text{-phen})$ in the mixed epoxy system of bisphenol A/novalac and DGEBA resin (0.05 mm thin film) containing a triarylsulfonium hexafluoroantimonate photoinitiator as a function of UV irradiation time: (A) 0 s, (B) 15 s, (C) 30 s and (D) 60 s. The emission spectra are uncorrected for photomultiplier response and vertically displaced for clarity. Excitation wavelength is 420 nm in each case. (b) Plot of emission intensity at the MLCT band maximum of *fac*-$ClRe(CO)_3(4,7\text{-}Ph_2\text{-phen})$ as a function of UV irradiation time. (Reprinted, with permission, from Ref. [75].)

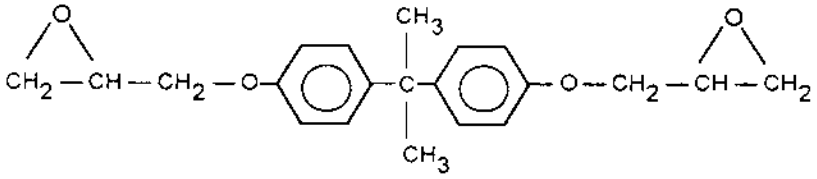

diglycidyl ether of bisphenol A (DGEBA)

The spectra reveal an emission band centered at 460 nm which is observed prior to UV irradiation; this is evident even in the absence of added organometallic probe complex and has been attributed to Raman scattering arising from the resin itself [74]. A long wavelength emission band is also initially observed as a shoulder at 582 nm and this feature subsequently intensifies greatly upon UV exposure and appears as a maximum at 522 nm; this band has been identified as the ^{3}MLCT emission of *fac*-Re(CO)$_3$(4,7-Ph$_2$-phen). However, both the increase in emission intensity and the hypsochromic shift (1945 cm^{-1}) of the long wavelength band are substantially larger than that observed for the same Re complex in the acrylate mixtures (160–672 cm^{-1}, see Table 4). Moreover, the emission lifetime of *fac*-ClRe(CO)$_3$(4,7-Ph$_2$-phen) in this cured epoxy resin is 6.4 μs, which is appreciably longer than the 2.5 μs recorded in the 1:1 TMPTA + PMMA acrylate system.

Once again, the increases in emission intensity and lifetime of the organometallic complex can be related to a reduction in the nonradiative decay pathways as the epoxy material polymerizes and forms a rigid network. The observed rigidochromic shifts, though, are very much greater than seen in the acrylate-based systems. However, it should be recognized that the cured epoxy matrix is highly polar [$\delta = 9.7–10.9$ (cal cm^{-3})$^{1/2}$] [81] and will substantially influence the excited state of the probe complex. In comparison, the dipolar interactions in acrylates such as the TMPTA + PMMA mixtures described above will be considerably less because their polymerized networks are not as polar [$\delta \sim 9.4$ (cal cm^{-3})$^{1/2}$] [81].

4. Thermosetting polymers

4.1. Epoxy-based resins

Epoxy resins exhibit an excellent combination of mechanical and electrical properties and are suitable for various electronic applications as in adhesives, electrical moldings, matrix materials for dielectrics, protective coatings and encapsulants [82–85]. In each of these applications, however, it is desirable to monitor the chemical and physical changes accompanying the curing mechanism. Consequently, a number of spectroscopic techniques have been used to characterize polymerization changes in epoxy resins, generally represented by the gelation and vitrification stages. These have included infrared spectroscopy, dynamic mechanical spectrometry and gel fraction methods [86]. Additionally, electron paramagnetic resonance spectroscopy has been employed to study the microstructure in polymeric networks of an epoxy resin using nitroxide spin labels and spin probes [87].

There are now numerous reports that have described the use of various fluorescence probes to monitor changes in matrix viscosity and morphology during thermal cross-linking reactions [49–52,55–71,79,80,88–90]. The organic dye, auramine O, was one of the earliest of these systems, having been found to be sensitive to the host polymer rigidity [91]. Here, the probe molecule undergoes internal quenching when the two phenylene groups in the excited state lose their coplanarity and this energy transfer process is hindered by the viscosity of the medium. Indeed, as in the probe studies of photopolymerization [53,54], the reduction or elimination of nonradiative relaxation pathways has been utilized in a number of fluorescence probe systems [49–52,55–63]. In some instances, however, an added molecule can serve as a spectroscopic probe. For example, the cure of diglycidyl ether of butanediol has been monitored using *trans*-diaminostilbene as a reactive label [92]. Both the ultraviolet absorption and fluorescence spectra of the stilbene undergo bathochromic shifts as the primary amines are converted to tertiary amines in this polymerization reaction.

Recently, the *fac*-$XRe(CO)_3(\alpha,\alpha'$-diimine) complexes have been shown to act as probes in epoxide systems, including the cycloaliphatic epoxy/anhydride resin formulated with (3,4-epoxycyclohexyl)methyl-3,4-epoxycyclohexylcarboxylate and *cis*-cyclohexanedicarboxylic anhydride which is cured with the addition of *N*-benzyldimethylamine [93,94]. The rhenium complexes are soluble and stable in this resin and exhibit no signs of thermal degradation, even during cure sequences performed as high as 413 K.

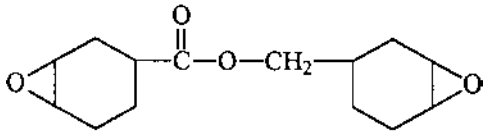

cycloaliphatic epoxy

Representative emission spectra recorded from *fac*-$ClRe(CO)_3(4,7\text{-}Ph_2\text{-phen})$ in the cycloaliphatic epoxy/anhydride system are illustrated in Fig. 11. Three stages of the polymerization are depicted: before curing, following curing at 393 K for 30 min and after curing at 393 K for 60 min. Dual emission features are observed at 480 and 610 nm prior to the reaction and then the relative intensity of the higher energy band diminishes greatly upon curing. This emission feature is assigned to both fluorescence and scattered light arising from the resin itself as it is observed in the absence of any added organometallic probe and its energy position is also dependent on the excitation wavelength. On the other hand, the lower energy emission band is only observed when the rhenium complex is incorporated and is clearly attributed to ^{3}MLCT emission. This long wavelength emission increases in intensity by a factor of 10 during the curing processes. Importantly, the band also energy shifts during the cross-linking reaction; it appears at 610 nm prior to the cure and moves to 556 nm once the cure is complete (after heating at 393 K for 180 min), corresponding to a hypsochromic shift of 1592 cm^{-1}. Table 5 summarizes the absorption and emission data recorded for the *fac*-$XRe(CO)_3(\alpha,\alpha'$-diimine) series in the uncured and cured cycloaliphatic epoxy/anhydride resins [93]. It can be seen that the rigidochromic shifts range from 764 to 1633 cm^{-1}, depending on the particular probe complex. Recently, it has been

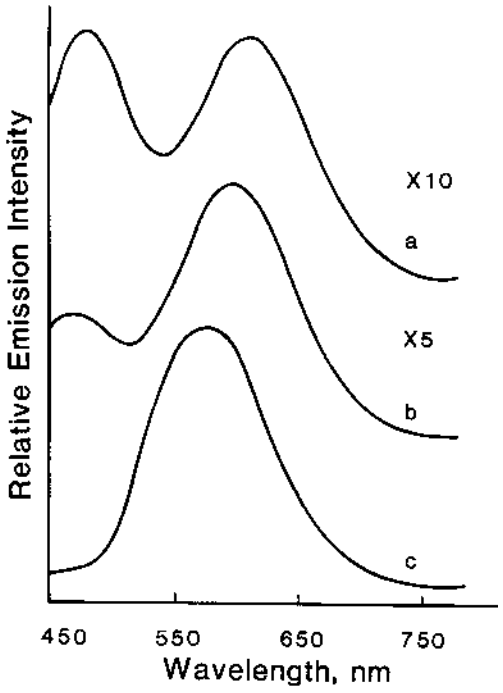

Fig. 11. Emission spectra of (0.008% by weight) *fac*-$ClRe(CO)_3(4,7\text{-}Ph_2\text{-phen})$ in the cycloaliphatic epoxy/anhydride resin at 293 K: (a) before curing; (b) partially cured by heating at 393 K for 30 min; and (c) cured by heating at 393 K for 60 min. The emission spectra are uncorrected for photomultiplier response; excitation wavelength is 400 nm in each case. Intensities of spectra (a) and (b) have been scaled $\times 10$ and $\times 5$, respectively. (Reprinted, with permission, from Ref. [93].)

demonstrated that in the case of the X = I derivative the nature of the lowest energy excited state is predominantly XLCT rather than MLCT [95]; the substantially lower ΔE_{em} value appears to reflect this change in the excited state character.

Excitation spectra have been recorded for the rhenium complexes in the epoxy resin while monitoring emission at the ^{3}MLCT maxima; a representative spectrum is shown in Fig. 12. Similar excitation spectra have been obtained from *fac*-$ClRe(CO)_3(4,7\text{-}Ph_2\text{-phen})$ in deoxygenated methylene chloride solution, confirming the ^{3}MLCT assignment of the lowest energy emission band. Emission quantum yields and lifetimes have also been measured for the *fac*-$XRe(CO)_3L$ series and are shown in Table 6. Included are photophysical deactivation rate constants, derived according to Eqs. (1) and (2) (here it is assumed that the emitting state is formed with unity efficiency) [21,45]. Significantly, it can be seen that for each probe complex the nonradiative decay constant (k_{nr}) is decreased by at least an order of magnitude, whereas the radiative rate constant (k_r) is relatively unchanged. This observation is in agreement with the above discussion for the methyl methacrylate polymerization, where it was concluded that k_{nr} decreases as polymer viscosity is increased and the free volume is reduced [79,80].

The energy position of the emission maximum of *fac*-ClRe(CO)$_3$(4,7-Ph$_2$-phen) has been monitored as a function of cure time in the cycloaliphatic epoxy/anhydride resin and the results are illustrated in Fig. 13 [94]. It can be seen that during the cure sequence the energy of the ^{3}MLCT emission from the probe increases sharply and subsequently reaches a plateau after about 60 min of cure time. Dynamic mechanical analyses of the resin have been carried out in a parallel plate geometry and the resulting stress amplitude and phase angle have been measured, leading to a determination of the dynamic moduli (G' and G'') which are measures of the stress/strain ratio during deformation [96]. The complex shear modulus and viscosity have been derived, according to Eqs. (4) and (5),

$$G^* = [(G')^2 + (G'')^2]^{1/2} \quad (4)$$

$$\eta^* = G^*/\omega \quad (5)$$

where G^* is the complex shear modulus, G' is the storage or elastic modulus, G'' is the loss modulus, η^* represents the complex viscosity and ω is the angular frequency (rad s^{-1}). The dynamic moduli and complex viscosity results for the cycloaliphatic epoxy/anhydride resin are depicted in Fig. 14. The t_{gel} value represents the time to gelation based on the dynamic moduli crossover ($G' = G''$) and is estimated at 18 min [97–99]. The t_{vit} value denotes the time to vitrification based on the second inflection point in the η^* data and is found at approximately 28 min.

Clearly, the emission band maximum of *fac*-ClRe(CO)$_3$(4,7-Ph$_2$-phen) is significantly influenced by the changing physical properties of the cycloaliphatic epoxy/anhydride material. Throughout the curing process the epoxy resin forms a cross-linked three-dimensional network of increasing molecular weight and its viscosity increases by approximately five orders of magnitude, from about 10 Pa s to almost 10^6 Pa s (Fig. 14a). Similarly, the energy position of the ^{3}MLCT emission

Table 5
Absorption and emission maxima of the MLCT bands observed from *fac*-XRe(CO)$_3$L complexes in deoxygenated methylene chloride and the cycloaliphatic epoxy/anhydride system at 293 K[a]

Complex	λ_{abs} (nm)	λ_{em} (nm)			
	CH_2Cl_2	CH_2Cl_2	Uncured epoxy	Cured[b] epoxy	ΔE^c_{em} (cm^{-1})
fac-ClRe(CO)$_3$(phen)	378	591	592	543	1524
fac-ClRe(CO)$_3$(4-Me-phen)	372	587	575	543	1025
fac-ClRe(CO)$_3$(4,7-Ph$_2$-phen)	381	598	610	556	1592
fac-BrRe(CO)$_3$(4,4′-Me$_2$-bpy)	382	587	585	534	1633
fac-IRe(CO)$_3$(4,7-Ph$_2$-phen)	410	602	608	581	764

[a] Data taken from Ref. [93]. Emission spectra are uncorrected for wavelength variations in photomultiplier response; excitation wavelength is 400 nm.
[b] Cured by heating at 393 K for 180 min; observed emission intensity is ca. 10-fold greater than uncured sample.
[c] Energy difference between observed emission bands of the organometallic probes in uncured and cured epoxy samples.

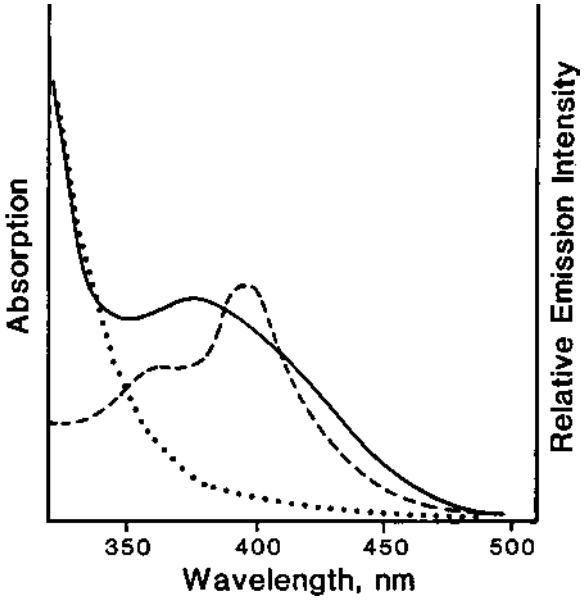

Fig. 12. Electronic absorption (——) and excitation (– – –) spectra of 0.008% (by weight) *fac*-$ClRe(CO)_3$(4,7-Ph_2-phen) in the cycloaliphatic epoxy/anhydride resin at 293 K. The electronic absorption spectrum (· · ·) of the uncured epoxy/anhydride resin without the incorporation of the organometallic complex is also shown. The excitation spectrum was recorded with emission monitored at 610 nm. (Reprinted, with permission, from Ref. [93].)

band of the probe complex undergoes a substantial blue shift (up to 1633 cm^{-1}, see Table 5) when the epoxy resin is cured. The S-shaped dependence exhibited by the emission data (Fig. 13) essentially occurs in these stages; on initial heating there is

Table 6
Photophysical parameters for *fac*-$XRe(CO)_3L$ complexes in the uncured and cured cycloaliphatic/anhydride epoxy system at 293 K[a]

Complex	Cure state[b]	ϕ_e^c	τ_e (ns)	k_r (s^{-1})	k_{nr} (s^{-1})
fac-$ClRe(CO)_3$(4,7-Ph_2-phen)	Uncured	0.042	280	1.5×10^5	3.4×10^6
	Cured	0.44	4100	1.1×10^5	1.3×10^5
fac-$ClRe(CO)_3$(4-Me-phen)	Uncured	0.039	306	1.3×10^5	3.1×10^6
	Cured	0.56	2360	2.4×10^5	1.8×10^5
fac-$IRe(CO)_3$(4,7-Ph_2-phen)	Uncured	0.048	1049	4.6×10^4	9.1×10^5
	Cured	0.56	8100	6.9×10^4	5.4×10^4
fac-$BrRe(CO)_3$(4,4′-Me_2-bpy)	Uncured	0.035	77	4.5×10^5	1.3×10^7
	Cured	0.37	600	6.2×10^5	1.0×10^6

[a] Data taken from Ref. [94]. Excitation wavelength is 400 nm.
[b] Cured samples were heated at 393 K for 180 min.
[c] Obtained from corrected emission spectra using emission quantum yield of *fac*-$ClRe(CO)_3$(phen) in deoxygenated CH_2Cl_2 as a calibrant (Ref. [21]).

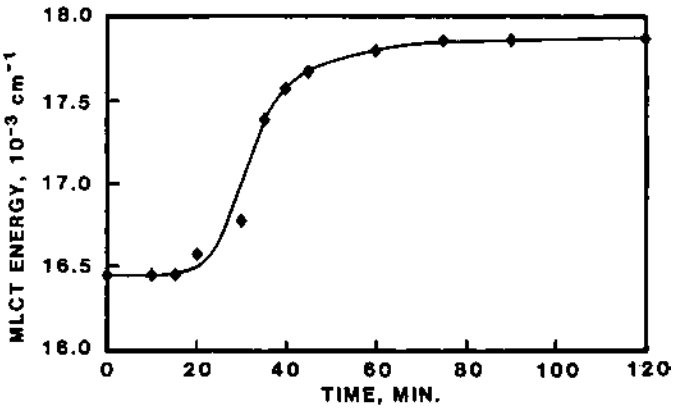

Fig. 13. Energy position of the uncorrected ^{3}MLCT emission band maximum of *fac*-ClRe(CO)$_3$(4,7-Ph$_2$-phen) in the cyloaliphatic epoxy/anhydride resin as a function of time at the isothermal temperature of 393 K. The spectra were recorded at 293 K following excitation at 400 nm. (Reprinted, with permission, from Ref. [94].)

no change in the ^{3}MLCT band position, then this is followed by a sharp increase in the energy of the emission band accompanying the onset of the gelation, and finally the changes become more gradual and a plateau is reached after vitrification has taken place. From the probe data of Fig. 13 it can be estimated that t_{gel} is in the range 18–25 min (indicated by the sharp change in slope of emission energy against cure time) and t_{vit} is at about 40–45 min (from the second slope change on the emission curve). These times are somewhat longer than the values obtained from the dynamic mechanical analyses, but one should recognize that in these experiments there is a lag time in the emission measurements compared to the rheological data.

Results determined for the *fac*-ClRe(CO)$_3$(4,7-Ph$_2$-phen) probe in related room temperature curing epoxy systems involving diglycidyl ether of bisphenol A (DGEBA) are, therefore, of interest in this regard. Fig. 15 illustrates the results of measurements of ^{3}MLCT intensity and η^* from DGEBA resins containing the rhenium probe and either polymercaptan or amine curing agents [94]. Here, determining the emission intensity at a constant wavelength was found to provide a most valuable in situ method of monitoring the polymerization. Clearly, in both the DGEBA/polymercaptan and DGEBA/amine resins, the ^{3}MLCT emission intensity and complex viscosity data exhibit an analogous dependency with the curing time.

The close relationship between the ^{3}MLCT energy of *fac*-ClRe(CO)$_3$(4,7-Ph$_2$-phen) and η^* of the resin has been further explored in the cycloaliphatic epoxy/anhydride material via a series of temperature dependence measurements [94]. Fig. 16 depicts data recorded for both the ^{3}MLCT energy position of the probe complex and η^* of the neat cycloaliphatic epoxy resin (without anhydride or added amine) at temperatures between 210 and 300 K. As the epoxy freezes the viscosity rises by over five orders of magnitude and the probe emission blue shifts substantially; in

each case the results display a reversed S-shaped function. Obviously, there is a strong correlation between the ^{3}MLCT and η^* data and this is exemplified by the semi-log plot shown in Fig. 17. Importantly, the energy shifts in emission of the organometallic complex are sensitive over such large changes in the resin viscosity, thereby providing a spectroscopic probe throughout the polymerization.

5. The luminescence rigidochromic effect

Clearly, the characteristics of luminescence rigidochromism can be very useful in designing spectroscopic probes to monitor viscosity changes in both thermal and photochemical polymerization reactions. Questions do remain, however, concerning the underlying causes of this phenomenon. In order to understand more about this effect the electronic absorption and emission results obtained for the range of photosensitive and thermosetting polymers are compiled in Table 7. This comparison is revealing as it is immediately apparent that the absorption maxima of the

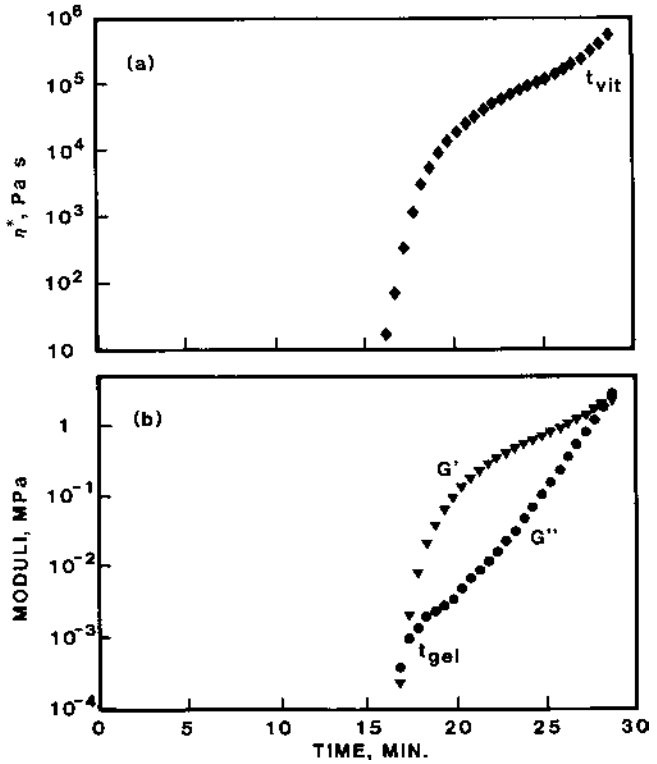

Fig. 14. (a) Complex viscosity (η^*) and (b) dynamic moduli (G' and G'') data in the cycloaliphatic epoxy/anhydride resin as a function of cure time at 393 K. Here t_{gel} and t_{vit} represent the times to gelation and vitrification, respectively. (Reprinted, with permission, from Ref. [94].)

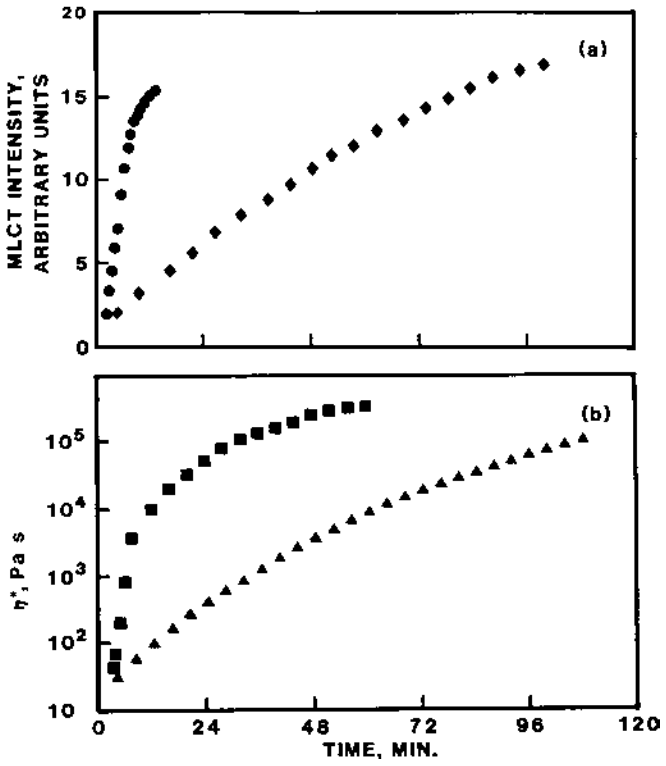

Fig. 15. (a) Intensity of ^{3}MLCT emission at 600 nm of *fac*-ClRe(CO)$_3$(4,7-Ph$_2$-phen) in the (●) DGEBA/polymercaptan and (◆) DGEBA/amine epoxy resins and (b) complex viscosity (η^*) data from (■) DGEBA/polymercaptan and (▲) DGEBA/amine epoxy resins as a function of time at the isothermal cure temperature of 293 K. Emission data recorded at 293 K following excitation at 400 nm. (Reprinted, with permission, from Ref. [94].)

probe complexes exhibit relatively small hypsochromic shifts upon increasing the matrix rigidity. In contrast, the MLCT emission bands are subjected to much more substantial hypsochromic shifts when the environment becomes rigid. A possible reason for this apparent decoupling between the absorption and emission behavior is that the ^{1}MLCT state that is reached on absorption is extremely short lived and decays rapidly via efficient nonradiative relaxation to the ground state and effective intersystem crossings, whereas the emissive ^{3}MLCT state is relatively long lived [1,2,100]. Thus, changes in the rigidity of the matrix environment are much more able to influence the relaxed ^{3}MLCT level, as it is this state which is most susceptible to variations in dipole–dipole interactions with the solvent molecules.

Scheme 1 illustrates a representation of the varying effects of dipolar interactions that can occur between the ground state (GS) or ^{3}MLCT excited state and the local solvent dipoles in the medium. In the ground state the surrounding solvent molecules are readily able to orient about the complex to best accommodate its dipole moment. In a ^{3}MLCT excited state the dipole moment of a substituted metal

carbonyl complex can be understood to be reversed from that of the ground state [27,101], so immediately upon excitation its dipole moment will be destabilized by the environment, until the solvent molecules reorient to facilitate a more favorable interaction [19]. This relaxation process will take place readily in fluid solution, but will be significantly restrained in a more rigid environment. The net result will be a destabilization of the ^{3}MLCT excited state under rigid conditions compared to the nonrigid situation and, subsequently, a hypsochromic shift in the emission from that level (Fig. 18). Such variations in solvation can be anticipated to be much less influential on the short-lived ^{1}MLCT excited states and so it is reasonable to assume that the absorption transitions experience considerably smaller energy perturbations.

Another feasible interpretation is that the luminescence rigidochromic effect is related to differing amounts of excited state distortion in the fluid and rigid environments. Certainly, there are large distortions in the ^{3}MLCT excited state compared to the ground state in these metal carbonyl complexes [2], as evidenced

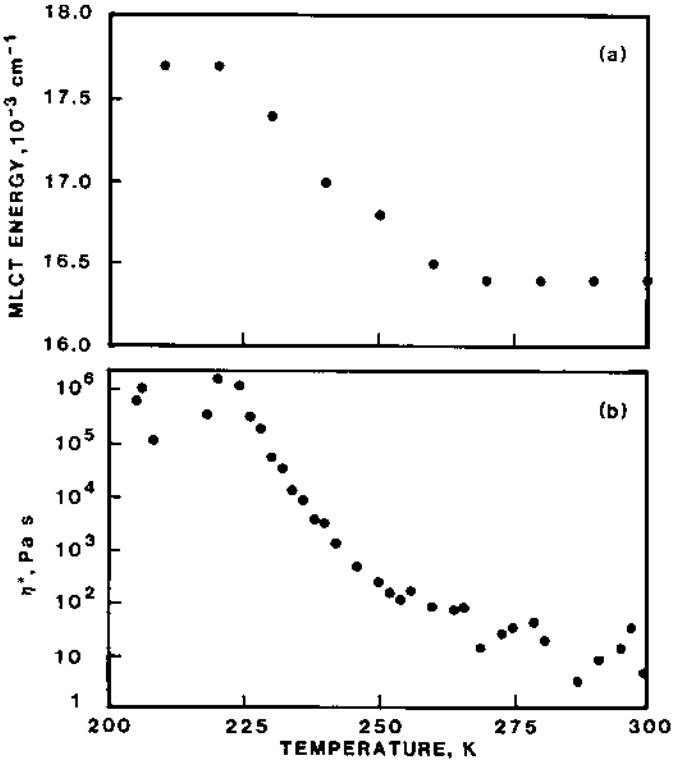

Fig. 16. (a) Energy position of the uncorrected ^{3}MLCT emission band maximum of *fac*-ClRe(CO)$_3$(4,7-Ph$_2$-phen) and (b) complex viscosity (η^*) changes as a function of temperature in the neat cycloaliphatic epoxy resin. The excitation wavelength is 400 nm for the data in (a). (Reprinted, with permission, from Ref. [94].)

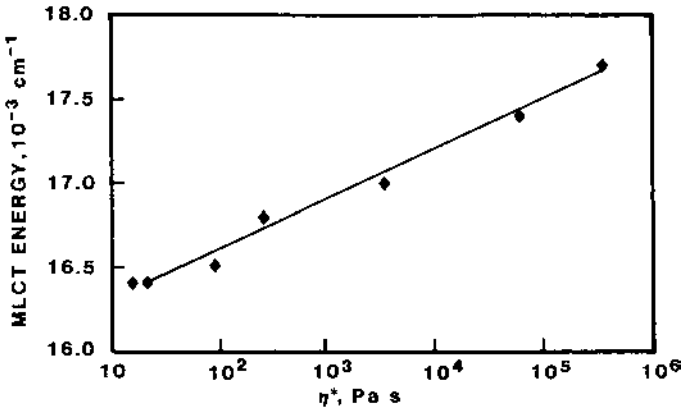

Fig. 17. Plot of the energy position of the uncorrected ^{3}MLCT emission band maximum of *fac*-$ClRe(CO)_3$(4,7-Ph_2-phen) against the determined complex viscosity (η^*) values of the neat cycloaliphatic epoxy resin. Data taken from Fig. 16 between 220 and 273 K. (Reprinted, with permission, from Ref. [94].)

by the sizeable energy gaps between the emission and excitation spectra (Figs. 11 and 12). If the amount of excited state distortion is somewhat lower in a rigid matrix than in fluid solution then this would produce a hypsochromic shift in the emission band. Indeed, such a rationale has recently been suggested for $Cu_4I_4py_4$ and related copper clusters, an unusual example of molecules exhibiting rigidochromism but not solvatochromism in their luminescence from a cluster-centered excited state [102]. In the tungsten and rhenium organometallic systems it is likely that excited state destabilization and distortion both occur during the polymerization processes.

Table 7
Energy shifts observed at the MLCT absorption (ΔE_{abs}) and emission (ΔE_{em}) maxima for the *fac*-$XRe(CO)_3L$ and $W(CO)_4L$ complexes upon curing in thermosetting and photosensitive polymers[a]

Complex	Resin material[b]	ΔE_{abs} (cm^{-1})	ΔE_{em} (cm^{-1})
fac-$ClRe(CO)_3$(phen)	Thermosetting epoxy		1524
fac-$ClRe(CO)_3$(4-Me-phen)	Thermosetting epoxy	73	1025
fac-$ClRe(CO)_3$(4,7-Ph_2-phen)	Thermosetting epoxy	211	1592
	Thermosetting DGEBA epoxy		711
	Photosensitive epoxy		1945
	Photosensitive acrylate[c]		432
fac-$BrRe(CO)_3$(4,4′-Me_2-bpy)	Thermosetting epoxy	292	1633
fac-$IRe(CO)_3$(4,7-Ph_2-phen)	Thermosetting epoxy	369	764
$W(CO)_4$(4-Me-phen)	Photosensitive acrylate[c]		653

[a] Data compiled from Refs. [72–75,93,94].
[b] Thermosetting epoxy system is cycloaliphatic epoxy/anhydride mixture, unless otherwise stated.
[c] Composition is 1:1 TMPTA/PMMA (by weight).

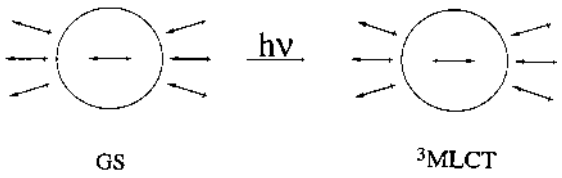

Scheme 1.

6. Conclusion

Several organometallic complexes which are emissive from low-lying ^{3}MLCT excited states have been employed as visible spectroscopic probes to monitor a variety of thermal and photochemical polymerizations. The luminescence properties of the probe molecules have been effectively correlated with spectroscopic (FTIR) and rheological (viscosity and dynamic moduli) measurements of the resin during the curing process. It has been shown that the luminescence rigidochromic characteristics of these organometallic probe complexes provide a new in situ way of determining the cure state and cure kinetics of several epoxy- and acrylate-based materials.

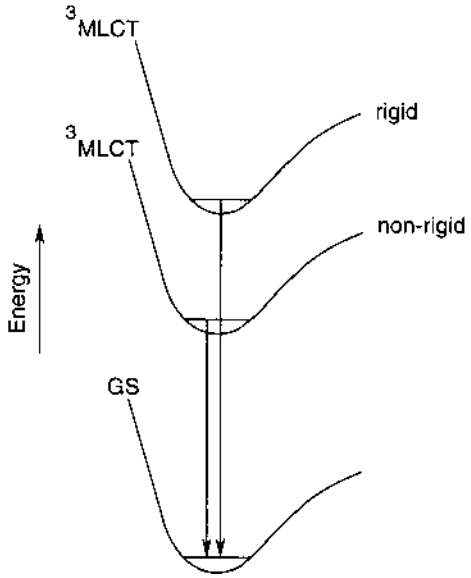

Fig. 18. Schematic representation of the emission from the ^{3}MLCT excited state in rigid and nonrigid environments. (Reprinted, with permission, from Ref. [72].)

Acknowledgements

Gratitude is extended to IBM Corp., the Petroleum Research Fund, administered by the American Chemical Society, and the Division of Chemical Sciences, Office of Basic Energy Sciences, Office of Energy Research, US Department of Energy (Grant DE-FG02-89ER14039) for funding the author's research which is cited in this review.

Appendix A. Abbreviations

ATR	attenuated total reflectance
biquin	2,2′-biquinoline
bpy	2,2′-bipyridine
4,4′-bpy	4,4′-bipyridine
5-Br-phen	5-bromo-1,10-phenanthroline
5-Cl-phen	5-chloro-1,10-phenanthroline
DGEBA	diglycidyl ether of bisphenol A
en	ethylenediamine
EPA	ether/isopentane/ethanol (5:5:2 by volume)
FTIR	Fourier transform infrared
LF	ligand field
MCD	magnetic circular dichroism
MLCT	metal-to-ligand charge transfer
4,4′-Me_2-bpy	4,4′-dimethyl-2,2′-bipyridine
4-Me-phen	4-methyl-1,10-phenanthroline
5-Me-phen	5-methyl-1,10-phenanthroline
2-Me-THF	2-methyl-tetrahydrofuran
5-NO_2-phen	5-nitro-1,10-phenanthroline
phen	1,10-phenanthroline
phen-5,6-dione	1,10-phenanthroline-5,6-dione
4,7-Ph_2-phen	4,7-diphenyl-1,10-phenanthroline
PMMA	poly(methyl methacrylate)
R-dab	1,4-diaza-1,3-butadiene
R-pyca	pyridine-2-carbaldehyde imine
RR	resonance Raman
TMPTA	trimethylolpropane triacrylate
η^*	complex viscosity
G^*	complex modulus
G'	storage modulus
G''	loss modulus
k_{nr}	nonradiative decay rate constant
k_r	radiative decay rate constant
λ_{abs}	absorption maximum
λ_{em}	emission maximum
v_f	polymer free volume

v_o	van der Waals volume
ω	angular frequency
ϕ_e	emission quantum yield
τ_e	emission lifetime
t_{gel}	time to gelation
t_{vit}	time to vitrification

References

[1] G.L. Geoffroy, M.S. Wrighton, Organometallic Photochemistry, Academic Press, New York, 1979.
[2] A.J. Lees, Chem. Rev. 87 (1987) 711.
[3] H. Bock, H. tom Dieck, Angew. Chem. Int. Ed. Engl. 5 (1966) 520.
[4] H. Saito, J. Fujita, K. Saito, Bull. Chem. Soc. Jpn. 41 (1968) 863.
[5] J. Burgess, J. Organomet. Chem. 19 (1969) 218.
[6] H. tom Dieck, I.W. Renk, Angew. Chem. Int. Ed. Engl. 9 (1970) 793.
[7] D. Walther, Z. Anorg. Allg. Chem. 396 (1973) 46.
[8] D. Walther, J. Prakt. Chem. 316 (1974) 604.
[9] M.S. Wrighton, D.L. Morse, J. Organomet. Chem. 97 (1975) 405.
[10] J. Burgess, J.G. Chambers, R.I. Haines, Trans. Met. Chem. (Weinheim, Ger.) 6 (1981) 145.
[11] A.J. Lees, A.W. Adamson, J. Am. Chem. Soc. 104 (1982) 3804.
[12] D.M. Manuta, A.J. Lees, Inorg. Chem. 22 (1983) 3825.
[13] A.J. Lees, J.M. Fobare, E.F. Mattimore, Inorg. Chem. 23 (1984) 2709.
[14] J.A. Connor, C. Overton, N. El Murr, J. Organomet. Chem. 277 (1984) 277.
[15] E.S. Dodsworth, A.B.P. Lever, Chem. Phys. Lett. 112 (1984) 567.
[16] D.M. Manuta, A.J. Lees, Inorg. Chem. 25 (1986) 3212.
[17] W. Kaim, S. Kohlmann, Inorg. Chem. 25 (1986) 3306.
[18] W. Kaim, S. Kohlmann, S. Ernst, B. Olbrich-Deussner, C. Bessenbacher, A. Schulz, J. Organomet. Chem. 321 (1987) 215.
[19] E.S. Dodsworth, A.B.P. Lever, Inorg. Chem. 29 (1990) 499.
[20] P.N.W. Baxter, J.A. Connor, J. Organomet. Chem. 486 (1995) 115.
[21] M. Wrighton, D.L. Morse, J. Am. Chem. Soc. 96 (1974) 998.
[22] P.J. Giordano, S.M. Fredericks, M.S. Wrighton, D.L. Morse, J. Am. Chem. Soc. 100 (1978) 2257.
[23] D.M. Manuta, A.J. Lees, Inorg. Chem. 25 (1986) 1354.
[24] K.A. Rawlins, A.J. Lees, Inorg. Chem. 28 (1989) 2154.
[25] K.A. Rawlins, A.J. Lees, A.W. Adamson, Inorg. Chem. 29 (1990) 3866.
[26] M.M. Zulu, A.J. Lees, Inorg. Chem. 27 (1988) 3325.
[27] M.M. Glezen, A.J. Lees, J. Am. Chem. Soc. 111 (1989) 6602.
[28] A.J. Lees, Comm. Inorg. Chem. 17 (1995) 319.
[29] M.S. Wrighton, D.L. Morse, J. Organomet. Chem. 97 (1975) 405.
[30] R.W. Balk, D.J. Stufkens, A. Oskam, Inorg. Chim. Acta 28 (1978) 133.
[31] R.W. Balk, D.J. Stufkens, A. Oskam, Inorg. Chem. 19 (1980) 3015.
[32] P.C. Servaas, H.K. van Dijk, T.L. Snoeck, D.J. Stufkens, A. Oskam, Inorg. Chem. 24 (1985) 4494.
[33] H.K. van Dijk, P.C. Servaas, D.J. Stufkens, A. Oskam, Inorg. Chim. Acta 104 (1985) 179.
[34] D.J. Robbins, A. Thompson, J. Mol. Phys. 25 (1973) 1103.
[35] W.K. Smothers, M.S. Wrighton, J. Am. Chem. Soc. 105 (1983) 1067.
[36] J.V. Caspar, T.D. Westmoreland, G.H. Allen, P.G. Bradley, T.J. Meyer, W.H. Woodruff, J. Am. Chem. Soc. 106 (1984) 3492.
[37] P. Glyn, M.W. George, P.M. Hodges, J.J. Turner, J. Chem. Soc. Chem. Commun. (1989) 1655.
[38] D.R. Gamelin, M.W. George, P. Glyn, F.-W. Grevels, F.P.A. Johnson, W. Klotzbücher, S.L. Morrison, G. Russell, K. Schaffner, J.J. Turner, Inorg. Chem. 33 (1994) 3246.

[39] M.W. George, F.P.A. Johnson, J.R. Westwell, P.M. Hodges, J.J. Turner, J. Chem. Soc. Dalton Trans. (1993) 2977.
[40] I.P. Clark, M.W. George, F.P.A. Johnson, J.J. Turner, J. Chem. Soc. Chem. Commun. (1996) 1587.
[41] G.A. Crosby, K.W. Hipps, W.H. Elfring, J. Am. Chem. Soc. 96 (1974) 629.
[42] J.B. Birks, Photophysics of Aromatic Molecules, Wiley, London, 1970, p. 182.
[43] J. Saltiel, J. D'Agostino, E.D. Megarity, L. Metts, K.R. Neuberger, M.S. Wrighton, O.C. Zafiriou, Org. Photochem. 3 (1973) 1.
[44] G. Fischer, K.A. Muszkat, E. Fischer, J. Chem. Soc. B (1968) 1156.
[45] N.J. Turro, Modern Molecular Photochemistry, Benjamin-Cummings, Menlo Park, CA, 1978, p. 179.
[46] A.A. Gamble, in: D.R. Randell (Ed.), Radiation Curing of Polymers, Royal Society of Chemistry, London, 1987, p. 48.
[47] B. Klingert, M. Riediker, A. Roloff, Comm. Inorg. Chem. 7 (1988) 109.
[48] E. Reichmanis, F.L. Thompson, Chem. Rev. 89 (1989) 1273.
[49] F.W. Wang, R.E. Lowry, W.H. Grant, Polymer 25 (1984) 690.
[50] C.S.P. Sung, in: C.E. Hoyle, J.M. Torkelson (Eds.), Photophysics of Polymers, ACS Symposium Series 358, American Chemical Society, Washington, DC, 1987, p. 463.
[51] A. Stroeks, M. Shmorhun, A.M. Jamieson, R. Simha, Polymer 29 (1988) 467.
[52] P. Dousa, C. Konak, V. Fidler, K. Dusek, Polym. Bull. (Berlin) 22 (1989) 585.
[53] S.F. Scarlata, J.A. Ors, Polym. Commun. 27 (1986) 41.
[54] E.W. Meijer, R.J.M. Zwiers, Macromolecules 20 (1987) 332.
[55] R. Hayashi, S. Tazuke, C.W. Frank, Macromolecules 20 (1987) 983.
[56] R. Hayashi, S. Tazuke, C.W. Frank, Chem. Phys. Lett. 135 (1987) 123.
[57] S. Tazuke, R.K. Guo, R. Hayashi, Macromolecules 21 (1988) 1046.
[58] J. Paczkowski, D.C. Neckers, Macromolecules 24 (1991) 3013.
[59] L.W. Jenneskens, H.J. Verhey, H.J. van Ramesdonk, A.J. Witteveen, J.W. Verhoeven, Macromolecules 24 (1991) 4038.
[60] J. Paczkowski, D.C. Neckers, J. Polym. Sci. A: Polym. Chem. 31 (1993) 841.
[61] J.A.J. Burrows, G.W. Haggquist, R.D. Burkhart, Macromolecules 23 (1990) 988.
[62] F.M. Winnik, Macromolecules 23 (1990) 1647.
[63] G. Wang, L. Chen, M.A. Winnik, Macromolecules 23 (1990) 1650.
[64] I. Yamazaki, F.M. Winnik, M.A. Winnik, S. Tazuke, J. Phys. Chem. 91 (1987) 4213.
[65] P. Chandar, P. Somasundaran, N.J. Turro, Macomolecules 21 (1988) 950.
[66] F.M. Winnik, Macromolecules 22 (1989) 734.
[67] J. Naciri, R.G. Weiss, Macromolecules 22 (1989) 3928.
[68] A. Pattikottu, W.L. Mattice, Macromolecules 23 (1990) 867.
[69] O. Valdes-Aguilera, C.P. Pathak, D.C. Neckers, Macromolecules 23 (1990) 689.
[70] M. Wilhelm, C.-L. Zhao, Y. Wang, R. Xu, M.A. Winnik, J.-L. Mura, G. Riess, M.D. Croucher, Macromolecules 24 (1991) 1033.
[71] J.C. Song, D.C. Neckers, in: M.W. Urban, T. Provder (Eds.), Multidimensional Spectroscopy of Polymers, ACS Symposium Series 598, American Chemical Society, Washington, DC, 1995, p. 472.
[72] K.A. Rawlins, A.J. Lees, S.J. Fuerniss, K.I. Papathomas, Chem. Mater. 8 (1996) 1540.
[73] T.G. Kotch, A.J. Lees, S.J. Fuerniss, K.I. Papathomas, R.W. Snyder, Inorg. Chem. 30 (1991) 4871.
[74] T.G. Kotch, A.J. Lees, S.J. Fuerniss, K.I. Papathomas, R.W. Snyder, Polymer 33 (1992) 657.
[75] T.G. Kotch, A.J. Lees, S.J. Fuerniss, K.I. Papathomas, R.W. Snyder, Inorg. Chem. 32 (1993) 2570.
[76] A.K. Doolittle, J. Appl. Phys. 23 (1952) 236.
[77] G.E. Johnson, J. Chem. Phys. 63 (1975) 4047.
[78] T. Karstens, K. Koh, J. Phys. Chem. 84 (1980) 1871.
[79] R.O. Loutfy, Macromolecules 14 (1981) 270.

[80] R.O. Loutfy, in: M.A. Winnik (Ed.), Photophysical and Photochemical Tools in Polymer Science: Conformation, Dynamics, Morphology, NATO ASI Ser. C, 182, D. Reidel, Dordrecht, The Netherlands, 1986, p. 429.
[81] G. Salomon, in: R. Houwink, G. Salomon (Eds.), Adhesion and Adhesives, Elsevier, Amsterdam, 1962, p. 17.
[82] C.A. May, Y. Tanaka (Eds.), Epoxy Resins Chemistry and Technology, Marcel Decker, New York, 1973.
[83] L.H. Lee, Adhesive Chemistry, Plenum, New York, 1983.
[84] D.R. Randell (Ed.), Radiation Curing of Polymers, Royal Society of Chemistry, London, 1987.
[85] W.D. Callister, Materials Science and Engineering: An Introduction, Wiley, New York, 1991.
[86] J.B. Enns, J.K. Gillham, J. Appl. Polym. Sci. 28 (1983) 2567 and references cited therein.
[87] I.M. Brown, T.C. Sandreczki, Macromolecules 18 (1985) 2072.
[88] G. Oster, Y. Nishijima, in: B. Ke (Ed.), Newer Methods of Polymer Characterization, Wiley-Interscience, New York, 1964, p. 207.
[89] M.A. Winnik, in: M.A. Winnik (Ed.), Photophysical and Photochemical Tools in Polymer Science: Conformation, Dynamics, Morphology, NATO ASI Ser. C, 182, D. Reidel, Dordrecht, The Netherlands, 1986, p. 611.
[90] F.W. Wang, R.E. Lowery, W.J. Plummer, B.M. Fanconi, E. Wu, in: C.E. Hoyle, J.M. Torkelson (Eds.), Photophysics of Polymers, ACS Symposium Series 358, American Chemical Society, Washington, DC, 1987, p. 454.
[91] G. Oster, Y. Nishijima, J. Am. Chem. Soc. 78 (1956) 1581.
[92] C.S.P. Sung, R. Mathisen, Polymer 28 (1987) 941.
[93] T.G. Kotch, A.J. Lees, S.J. Fuerniss, K.I. Papathomas, Chem. Mater. 3 (1991) 25.
[94] T.G. Kotch, A.J. Lees, S.J. Fuerniss, K.I. Papathomas, Chem. Mater. 4 (1992) 675.
[95] B.D. Rossenaar, D.J. Stufkens, A. Vlček Jr., Inorg. Chem. 35 (1996) 2902.
[96] P. Sherman, Industrial Rheology, Academic Press, London, 1970, p. 24.
[97] C.-Y.M. Tung, P.J. Dynes, J. Appl. Polym. Sci. 27 (1982) 569.
[98] H.H. Winter, F.J. Chambon, Rheology 30 (1986) 367.
[99] M.S. Heise, G.C. Martin, J.T. Gotro, Polym. Eng. Sci. 30 (1990) 83.
[100] P. Glyn, F.P.A. Johnson, M.W. George, A.J. Lees, J.J. Turner, Inorg. Chem. 30 (1991) 354.
[101] P.J. Giordano, M.S. Wrighton, J. Am. Chem. Soc. 101 (1979) 2888.
[102] D. Tran, J.L. Bourassa, P.C. Ford, Inorg. Chem. 36 (1997) 439.